Journal of Alloys and Compounds 485 (2009) 493–496

Contents lists available at ScienceDirect

Journal of Alloys and Compounds

journal homepage: www.elsevier.com/locate/jallcom

Effect of excitation power density on the upconversion luminescence of LaF_3:Yb^{3+}, Er^{3+} nanocrystals

Yuqiu Qu[a,b], Xianggui Kong[a,*], Yajuan Sun[a], Qinghui Zeng[a], Hong Zhang[c]

[a] Changchun Institute of Optics, Fine Mechanics and Physics, Chinese Academy of Sciences, Changchun 130033, PR China
[b] Graduate School of Chinese Academy of Sciences, Beijing 100049, PR China
[c] Van't Hoff Institute for Molecular Sciences, University of Amsterdam, , Amsterdam, The Netherlands

ARTICLE INFO

Article history:
Received 29 April 2009
Accepted 31 May 2009
Available online 6 June 2009

Keywords:
Nanostructured materials
Optical properties
Optical spectroscopy

ABSTRACT

The upconversion fluorescent Yb^{3+}, Er^{3+} ions co-doped LaF_3 nanocrystals were synthesized and studied. The nanocrystals display green and red visible emissions under 980 nm near infrared excitation, which is suitable for biological application. The effect of excitation power density on the upconversion luminescence properties of nanocrystals are investigated detailed. Under lower pump power density irradiation, the upconversion luminescence shows a typical two photon involved process. When the pump power density turns to higher region, the dependence of upconversion emission intensity versus the excitation power density exhibits as the hysteresis loops which does not accord with the normal two-photon process. This phenomenon may be caused by the thermal effect which can increase the temperature of nanocrystals, and then enhance the visible emissions greatly.

1. Introduction

In recent years, considerable attention has been focused on the luminescent nanomaterials such as lanthanide doped nanocrystals due to their potential applications in display devices, lasers, optical amplifies, biological labels, and diagnostics and therapeutics [1–5]. The lanthanide ions doped nanocrystals can generate higher energy light from lower energy excitation via sequential absorption of photons or energy transfers, which is called upconversion process [6,7]. Compared with down-conversion fluorescent nanocrystals, the upconverting nanocrystals show higher photochemical stability, improved signal-to-noise ratio, increased tissue penetration and lower toxicity [8–10]. Hence, they are suitable for biological studies and clinical applications such as fluorescence imaging, immunoassay, and DNA detection [11–14]. The potential diagnostic and therapeutic applications of the upconverting nanocrystals on tumor also evoke the studies of the physical and chemical properties of these materials [15,16].

Up to now, the most efficient upconversion phosphors are Yb, Er or Yb, Tm co-doped fluorides [17]. These fluorides display some distinct advantages over the conventional host matrix owing to the very low phonon energy of their crystal lattices which can reduce the quenching of the excited state of rare earth ions [18]. So LaF_3 is a good host material for rare earth ions incorporation. And many works have been done to apply the upconverting LaF_3 nanocrystals on the biolabels, DNA detection and so on [19,20]. However, due to lower upconversion efficiency, it needs higher pump power than down-conversion process when the upconversion nanocrystals are used on biological and environmental samples. Therefore, the study of the impact of excitation power density on the fluorescent properties of these upconverting materials is important for the application of upconversion materials.

Herein, we report the upconversion luminescence properties of LaF_3:Yb^{3+}, Er^{3+} nanocrystals and investigate the effect of excitation power density on the upconversion luminescence of LaF_3:Yb^{3+}, Er^{3+} nanocrystals. The excitation power density plays a key role on the application of upconverting nanocrystals. A mezzo excitation power density should be chosen to avoid the effect of thermal damage.

2. Experimental

The LaF_3:Yb^{3+}, Er^{3+} nanocrystals were synthesized based on a reported procedure [21]. In a typical procedure, 3 mmol NaF, 12 mL of water, 9 mL of ethanol, and 3 mL oleic acid were mixed together under agitation to form a homogeneous solution, and the solution was heated to 75 °C for 1 h. When this water-ethanol mixed solution became homogeneous, 2.5 mL mixed solution of 0.85 mmol $LaCl_3{\cdot}6H_2O$, 0.12 mmol $YbCl_3{\cdot}6H_2O$ and 0.03 mmol $ErCl_3{\cdot}6H_2O$ was drop-by-drop added into the reaction vessel. And then the resulting product was stirred for 2 h. The product was separated by a high-speed centrifuge and washed with anhydrous ethanol for several times, and then the washed sample was dried under vacuum at ambient temperature.

X-ray diffraction (XRD) patterns were recorded with a X-ray diffractometer (Regaku D/max-rA) using Cu Kα radiation (λ = 1.5406 Å). The sizes and morphologies of LaF_3:Yb^{3+}, Er^{3+} nanocrystals were characterized by field emission scanning

* Corresponding author. Tel.: +86 431 86176313.
E-mail address: kongxg14@yahoo.com.cn (X. Kong).

0925-8388/$ – see front matter.
doi:10.1016/j.jallcom.2009.05.145

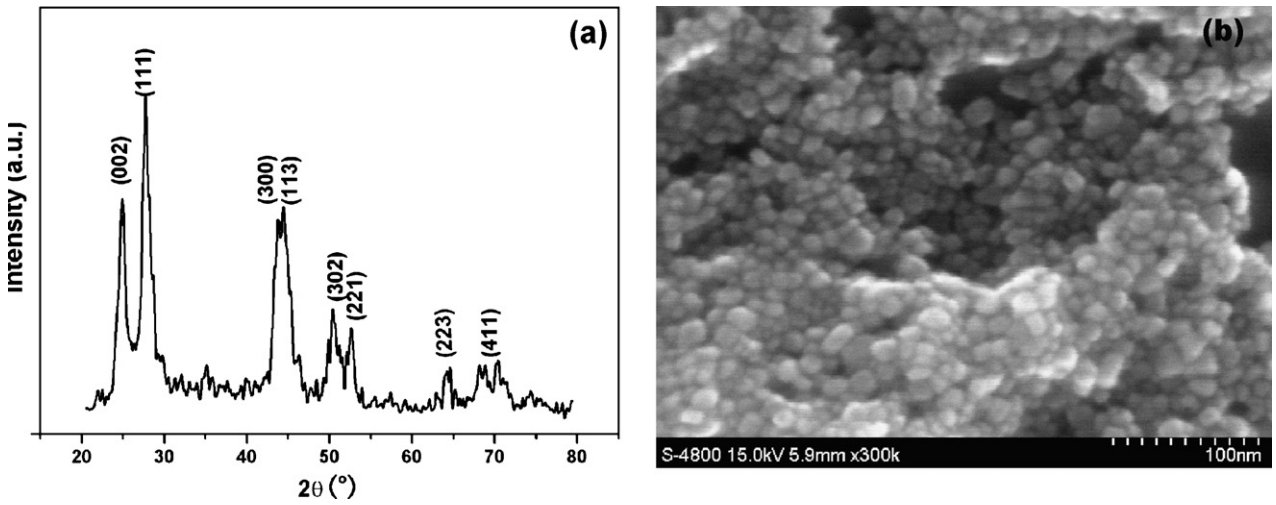

Fig. 1. (a) XRD pattern and (b) FESEM image of LaF_3:Yb^{3+}, Er^{3+} nanocrystals.

electron microscopy (FESEM, Hitachi, S-4800). The room temperature photoluminescence spectra were measured using a Jobin Yvon-LabRam Raman spectrometer and a Peltier air-cooled CCD detector. Samples were excited by a continuous wave semiconductor diode laser at 980 nm. And all the upconversion luminescence spectra were recorded at the same conditions.

3. Results and discussion

The XRD pattern of LaF_3:Yb^{3+}, Er^{3+} nanocrystals is presented in Fig. 1a. All the diffraction peaks correspond to the characteristic peaks of pure hexagonal phase LaF_3 (JCPDS card 72-1435). No other impurities have been found in the product. The broadening of peaks can be attributed to the small particle size of as-prepared nanocrystals. The average size of LaF_3:Yb^{3+}, Er^{3+} nanocrystals can be calculated to be 12 nm by using the Debye–Scherrer equation. Fig. 1b gives the SEM image of LaF_3:Yb^{3+}, Er^{3+} nanocrystals. As can be seen, the nanocrystals basically consist of spherical particles. The average particle size determined from the FESEM image is about 15 nm which is in reasonable agreement with that calculated from the XRD peaks.

Under continuous wave 980 nm semiconductor laser excitation, LaF_3:Yb^{3+}, Er^{3+} nanocrystals can exhibit the upconversion emission in the visible region at room temperature, as shown in Fig. 2 along with the energy level diagram of the Yb^{3+} and Er^{3+} ions. As can be seen, there are three emission peaks at 520, 540 and 654 nm for these nanocrystals under 980 nm near infrared excitation. The green emissions at 520 and 540 nm are assigned to $^2H_{11/2} \rightarrow {}^4I_{15/2}$ and $^4S_{3/2} \rightarrow {}^4I_{15/2}$ transitions, respectively. And the red emission at 654 nm can be assigned to $^4F_{9/2} \rightarrow {}^4I_{15/2}$ transition [22].

To better understand the populating mechanism of the $^2H_{11/2}$, $^4S_{3/2}$, and $^4F_{9/2}$ excited states following near infrared irradiation, the upconversion luminescence intensities of the green and red emissions (I_{em}) versus the excitation power density (I_p) should be performed. For upconversion process, the emission intensity (I_{em}) will be proportional to some power (n) of the excitation intensity (I_p) [23]:

$$I_{em} \propto I_p^n \quad \text{with } n = 2, 3 \ldots \tag{1}$$

where n is the number of infrared photons absorbed per visible photon emitted. But, the upconversion luminescence of LaF_3:Yb^{3+}, Er^{3+} nanocrystals will be influenced by the excitation power density in some degree. So the study on the effect of excitation power density is crucial for understanding of upconversion process.

Fig. 3 shows the logarithmic plots of the emission intensity as a function of excitation power which is at relatively low excitation densities for the green and red emissions of LaF_3:Yb^{3+}, Er^{3+} nanocrystals. By fitting the data points, the slope n of the curve can be determined. For the green emission, the value of n is determined

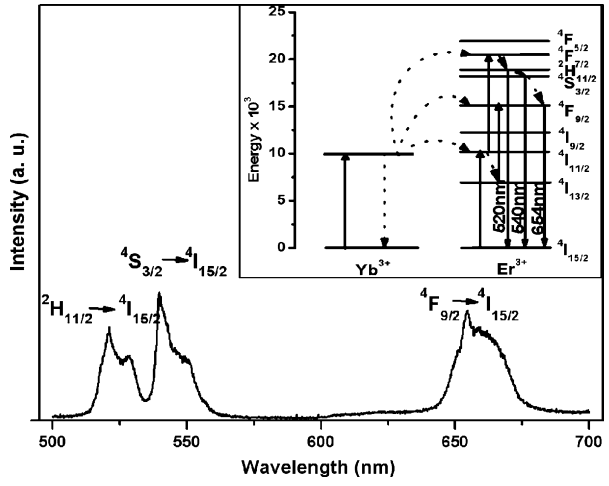

Fig. 2. The upconversion fluorescence emission spectrum of LaF_3:Yb^{3+}, Er^{3+} nanocrystals (λ_{exc} = 980 nm). Inset: the schematic energy level diagrams for Yb^{3+}, Er^{3+} system.

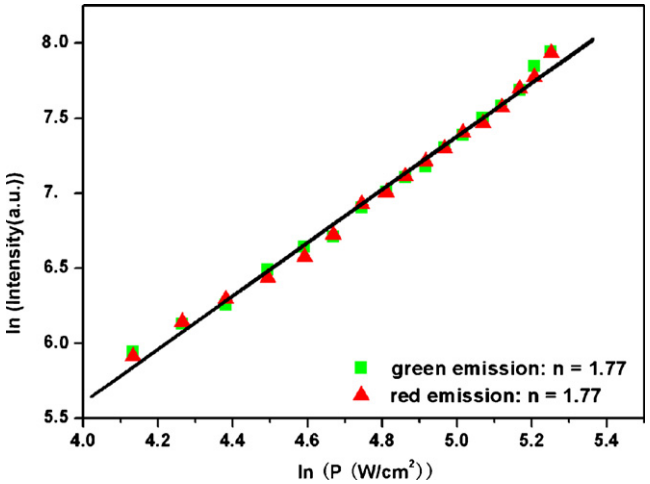

Fig. 3. Power dependence of the upconverted emissions of LaF_3:Yb^{3+}, Er^{3+} nanocrystals under low excitation power density.

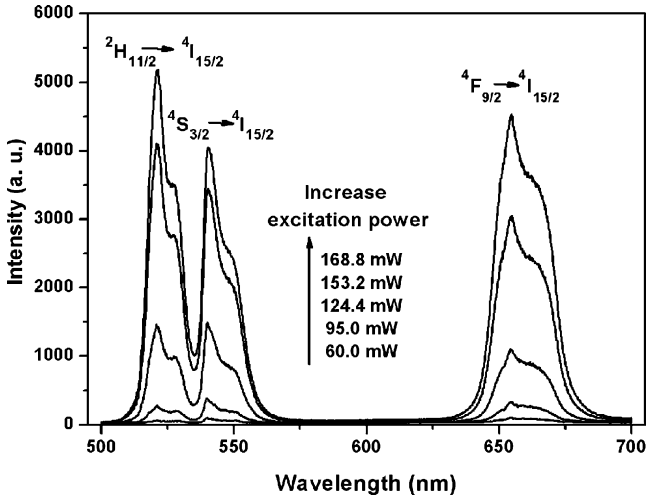

Fig. 4. The upconversion fluorescence emission spectra of LaF_3:Yb^{3+}, Er^{3+} nanocrystals under high excitation power density.

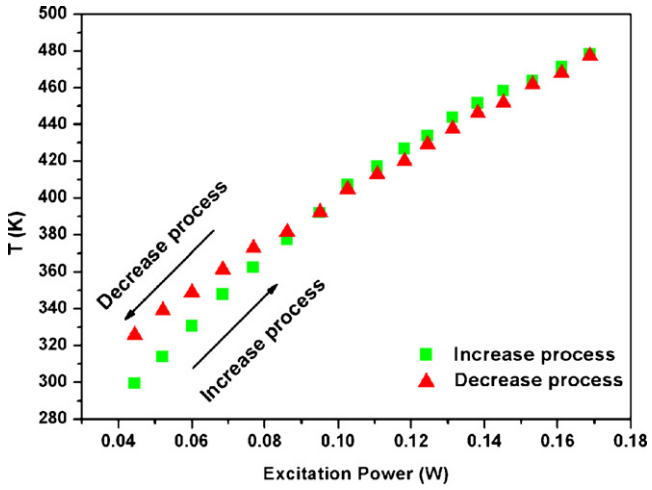

Fig. 6. The temperature as a function of pump power for LaF_3:Yb^{3+}, Er^{3+} nanocrystals.

to be 1.77, and for red emission, the value is 1.77 too. This indicates that two photons are involved in the upconversion process. The two photon upconversion mechanism is described in Fig. 2. Under 980 nm excitation, the Yb^{3+} ions in the $^2F_{5/2}$ state will transfer energy to Er^{3+} ions in the ground state, and then excite the ions to the $^4I_{11/2}$ state. Subsequently, another energy transfer process from Yb^{3+} ions in its excited state to Er^{3+} occurs and results in the population of the $^4F_{7/2}$ state of Er^{3+} [24]. Through nonradiative processes, the lower energy levels $^2H_{11/2}$, $^4S_{3/2}$ and $^4F_{9/2}$ are populated, and then green and red light are emitted by electron transmission from these states to ground state.

Because of the lower efficiency of the upconversion process [25], higher excitation power density will be used to obtain brighter visible light. As mentioned above, under lower excitation power density region, the upconversion process corresponds to the two photons mechanism. But when the excitation power density increases to a higher region, the intensities of green and red emission will increase rapidly with the increasing excitation power, as shown in Fig. 4. The dependence of upconversion emission intensity versus the excitation power is plotted in Fig. 5. It is clearly that the data points change non-linear. Sivakumar et al. [26] have demonstrated a newly hetero-looping-enhanced energy transfer upconversion process, which exhibits the power dependence similar to the case in Fig. 5. But, in this work, if we gradually decrease the excitation power after the irradiation, the intensities of all the emissions cannot go back to the original values. All data points in the decrease process are inclined to change linearly. And hysteresis loops are observed. So the hetero-looping-enhanced energy-transfer upconversion process cannot be applied to explain the phenomenon in Fig. 5.

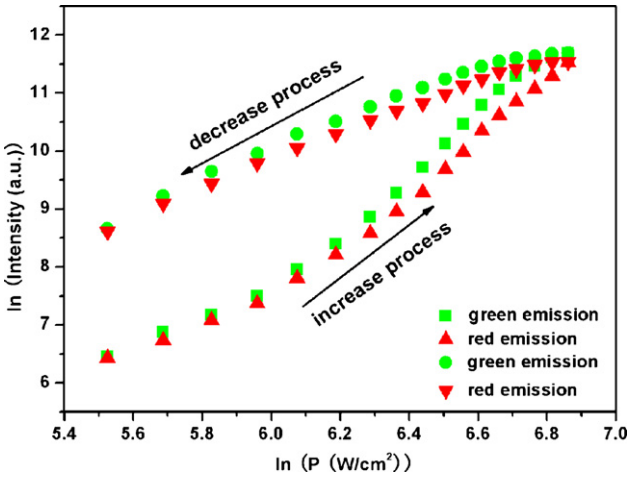

Fig. 5. Power dependence of the upconverted emissions of LaF_3:Yb^{3+}, Er^{3+} nanocrystals under high excitation power density.

In Fig. 4, we can observe that the green emission at 520 nm changes faster than others. The energy gap between the excited stats $^2H_{11/2}$ and $^4S_{3/2}$ is only several hundred wave numbers. The upper $^2H_{11/2}$ level is thermal populated owing to Boltzmann's distribution. So we used the relationship of two green emissions to calculate the temperature of the sample under high excitation power density [27]:

$$R_{HS} = \alpha \exp\left(\frac{-E_{HS}}{k_B T}\right) \quad (2)$$

where R_{HS} is the intensity ratio of $^2H_{11/2} \rightarrow {}^4I_{15/2}$ to $^4S_{3/2} \rightarrow {}^4I_{15/2}$, α is a constant, E_{HS} is the energy separation between the $^2H_{11/2}$ and the $^4S_{3/2}$ levels ($\sim$700 cm^{-1}), k_B is boltzmann's constant and T is the absolute temperature. In Fig. 6, we can see that under high excitation power irradiation, the temperature increases from room temperature to 480 K for the LaF_3:Yb^{3+}, Er^{3+} nanocrystals. In comparison, the temperature in the excitation power density increase process and decrease process are the same in the range of error. As mentioned above, the emission intensities cannot go back to the original values after irradiation. This phenomenon may be caused by the thermal effect. The samples are laser annealed, and then higher temperature changes the crystal field and capping ligands, so the upconversion luminescence properties will be influenced. Obviously, the red emission in the sample enhances more than the green emission. Based on the surface ligand dynamics of nanocrystals reported by Peng and co-workers [28], the surface ligand on the surface of nanocrystals will be more active on the surface with the increasing temperature, and then the interaction between the ligand and surface cations of nanocrystals will be intensified. The interaction will assist the nonradiative relaxation process. Thus the red emission which is dependent on the nonradiative relaxation will be enhanced as well as the interaction. Through this thermal effect we can tune the upconversion luminescence spectra. And based on these results, a moderate excitation power density can be selected for applications.

4. Conclusions

In summary, LaF_3:Yb^{3+}, Er^{3+} nanocrystals capped with oleic acid have been synthesized and the upconversion luminescence properties have been investigated. Bright green and red upconversion emissions have been generated with a 980 nm diode laser from the LaF_3:Yb^{3+}, Er^{3+} nanocrystals. The excitation power density plays an important role on the upconversion luminescence of LaF_3:Yb^{3+}, Er^{3+} nanocrystals. Under lower excitation power density, two photons are involved in the upconversion process. But under higher excitation power density, the upconversion emissions exhibit the power dependence that does not accord with the normal two photons process. Furthermore, the hysteresis loops of the emission intensity as a function of excitation power can be observed. The higher excitation power irradiation cause the thermal effect which increases the temperature of sample, so there may be some thermal damage on the crystal field and the capping ligand of LaF_3:Yb^{3+}, Er^{3+} nanocrystals. And then the upconversion luminescence properties change correspondingly.

Acknowledgements

This work was supported by NSFC of China (60601014 and 20603035) and exchange program between CAS of China and KNAW of the Netherlands.

References

[1] J.F. Suyver, A. Aebischer, D. Biner, P. Gerner, J. Grimm, S. Heer, K.W. Krämer, C. Reinhard, H.U. Güdel, Opt. Mater. 27 (2005) 1111.
[2] C.G. Morgan, S. Dad, A.C. Mitchell, J. Alloys Compd. 451 (2008) 526.
[3] A.M. Gobin, M.H. Lee, N.J. Halas, W.D. James, R.A. Drezek, J.L. West, Nano Lett. 7 (2007) 1929.
[4] P. Zhang, W. Steelant, M. Kumar, M. Scholfield, J. Am. Chem. Soc. 129 (2007) 4526.
[5] C.J. Sun, Z.H. Xu, B. Hu, G.S. Yi, G.M. Chow, J. Shen, Appl. Phys. Lett. 91 (2007) 191113.
[6] R. Scheps, Prog. Quant. Electr. 20 (1996) 271.
[7] F. Auzel, Chem. Rev. 104 (2004) 139.
[8] W.C.W. Chan, S.M. Nie, Science 281 (1998) 2016.
[9] D.K. Chatterjee, A.J. Rufaihah, Y. Zhang, Biomaterials 29 (2008) 937.
[10] J.A. Feijo, N. Moreno, Protoplasma 223 (2004) 1.
[11] F. van de Rijke, H. Zijlmans, S. Li, T. Vail, A.K. Raap, R.S. Niedbala, H.J. Tanke, Nat. Biotechnol. 19 (2001) 273.
[12] S.F. Lim, R. Riehn, W.S. Ryu, N. Khanarian, C.K. Tung, D. Tank, R.H. Austin, Nano Lett. 6 (2006) 169.
[13] L.Y. Wang, Y.D. Li, Chem. Commun. 24 (2006) 2557.
[14] M. Nyk, R. Kumar, T.Y. Ohulchanskyy, E.J. Bergey, P.N. Prasad, Nano Lett. 8 (2008) 3834.
[15] Y.J. Sun, Y. Chen, L.J. Tian, Y. Yu, X.G. Kong, J.W. Zhao, H. Zhang, Nanotechnology 18 (2007) 275609.
[16] Z.Q. Li, Y. Zhang, Nanotechnology 19 (2008) 345606.
[17] K.W. Krämer, D. Biner, G. Frei, H.U. Güdel, M.P. Hehlen, S.R. Lüthi, Chem. Mater. 16 (2004) 1244.
[18] J.W. Stouwdam, G.A. Hebbink, J. Huskens, F.C.J.M. van Veggel, Chem. Mater. 15 (2003) 4604.
[19] S. Sivakuma, P.R. Diamente, F.C.J.M. van Veggel, Chem. Eur. J. 12 (2006) 5878.
[20] A. Pich, F.B. Zhang, L. Shen, S. Berger, O. Ornatsky, V. Baranov, M.A. Winnik, Small 4 (2008) 2171.
[21] J.S. Wang, J. Hu, D.H. Tang, X.H. Liu, Z. Zhen, J. Mater. Chem. 17 (2007) 1597.
[22] D. Matsuura, Appl. Phys. Lett. 81 (2002) 4526.
[23] M. Pollnau, D.R. Gamelin, S.R. Luthi, H.U. Güdel, M.P. Hehlen, Phys. Rev. B 61 (2001) 3337.
[24] P.S. Golding, S.D. Jackson, T.A. King, M. Pollnau, Phys. Rev. B 62 (2000) 856.
[25] G.S. Yi, G.M. Chow, J. Mater. Chem. 15 (2005) 4460.
[26] S. Sivakumar, F.C.J.M. van Veggel, P.S. May, J. Am. Chem. Soc. 129 (2007) 620.
[27] X. Wang, X.G. Kong, Y. Yu, Y.J. Sun, H. Zhang, J. Phys. Chem. C 111 (2007) 15119.
[28] N. Pradhan, D. Reifsnyder, R.G. Xie, J. Aldana, X.G. Peng, J. Am. Chem. Soc. 129 (2007) 9500.